Available online at www.sciencedirect.com
ScienceDirect
Journal of Magnetic Resonance 187 (2007) 343–351
JMR Journal of Magnetic Resonance
www.elsevier.com/locate/jmr

Use of SPAM and FAM pulses in high-resolution MAS NMR spectroscopy of quadrupolar nuclei

Thomas J. Ball, Stephen Wimperis *

Department of Chemistry and WestCHEM, University of Glasgow, Glasgow G12 8QQ, UK

Received 15 March 2007; revised 18 May 2007
Available online 9 June 2007

Abstract

The merits of SPAM and FAM pulses for enhancing the conversion of triple- to single-quantum coherences in the two-dimensional MQMAS experiment are compared using ^{87}Rb (spin $I = 3/2$) and ^{27}Al ($I = 5/2$) NMR of crystalline and amorphous materials. Although SPAM pulses are more easily optimized, our experiments and simulations suggest that FAM pulses yield greater signal intensity in all cases. In conclusion, we argue that, as originally suggested, SPAM and FAM pulses are best implemented in phase-modulated whole-echo MQMAS experiments and that the use of SPAM pulses to record separate echo and antiecho data sets, which are then combined, generally yields lower signal-to-noise ratios.

Keywords: NMR; Solid-state NMR; MAS NMR; Composite pulses; MQMAS; STMAS; FAM; SPAM

1. Introduction

The acquisition of high-resolution NMR spectra of quadrupolar nuclei in solids has been facilitated by the introduction of the multiple-quantum magic angle spinning (MQMAS) [1] and satellite-transition magic angle spinning (STMAS) [2] techniques. These methods achieve complete refocusing of the second-order quadrupolar interaction by two-dimensional correlation under MAS conditions. This correlation is between a multiple-quantum transition (typically, $m_I = +3/2 \leftrightarrow -3/2$) and the directly observable central transition ($+1/2 \leftrightarrow -1/2$) in MQMAS and between satellite transitions (typically, $\pm 3/2 \leftrightarrow \pm 1/2$) and the central transition in STMAS. As the second-order quadrupolar broadenings of the coherences involved in each experiment differ by only a scaling factor under MAS, either technique can be used to yield an "isotropic" spectrum in which the effects of the first- and second-order quadrupolar interactions have been suppressed.

The main weakness of the MQMAS and STMAS experiments is that the mixing or conversion step, namely the conversion of multiple-quantum to central-transition coherences in MQMAS and of satellite- to central-transition coherences in STMAS, is very inefficient and, as a result, the overall sensitivity is poor. Several methods have been developed to improve the efficiency of the conversion process, mainly concentrating on MQMAS. These include RIACT (rotationally induced adiabatic coherence transfer) pulses [3], DFS (double frequency sweep) pulses [4], FAM (fast amplitude modulated) pulses [5], and HS (hyperbolic secant) pulses [6]. These all yield enhanced triple-quantum to central-transition coherence transfer and hence increased sensitivity for MQMAS.

Much recent activity in this area has focused on the SPAM (soft pulse added mixing) method [7] and its application to both MQMAS and double-quantum filtered (DQF) STMAS NMR [8–11]. Like the windowless FAM pulses [12], we view SPAM pulses as composite pulses [13,14], in this case consisting of an intense or "hard" radiofrequency pulse followed immediately by a "soft" pulse that acts as a selective 90° pulse on the central-transition ($+1/2 \leftrightarrow -1/2$). The relative phase of the two

* Corresponding author. Fax: +44 141 3304888.
E-mail address: s.wimperis@chem.gla.ac.uk (S. Wimperis).

1090-7807/$ - see front matter © 2007 Elsevier Inc. All rights reserved.
doi:10.1016/j.jmr.2007.05.020

components of a SPAM pulse is either 0° or 180° depending on whether the desired coherence transfer step results in a change in the sign of the coherence order p [7,8]. In addition, to yielding signal enhancement, the two versions of the SPAM pulse have also been reported to have the property that, when implemented into the echo and antiecho versions of the two-pulse MQMAS experiment, they yield very similar signal intensities [7,8]; this has led to the suggestion that combining the data from SPAM-echo and SPAM-antiecho experiments is a practical and effective method of recording MQMAS spectra with enhanced sensitivity [8].

The purpose of this paper is to compare SPAM pulses with FAM pulses as a means of enhancing the efficiency of the conversion step in MQMAS. We have chosen to use windowless FAM pulses in this comparison because they represent a "typical" and well-known signal enhancement technique for MQMAS and because they resemble SPAM pulses quite closely; it is not because we consider them to be superior to methods such as DFS or HS pulses. The comparison will be performed using ^{87}Rb (spin $I = 3/2$) and ^{27}Al ($I = 5/2$) NMR of crystalline and amorphous materials and using computer simulations. Finally, we will discuss optimal approaches to implementing SPAM pulses in two-dimensional MQMAS experiments.

2. Lineshapes and signal enhancement in MQMAS NMR

The simplest version of the MQMAS experiment consists of two pulses, one for excitation of triple-quantum and one for its subsequent conversion to observable single-quantum coherence [1]. This experiment, as shown in Fig. 1a, can be performed with phase cycling that selects one of two coherence pathways: the $0 \to -3 \to -1$ pathway or the $0 \to +3 \to -1$ pathway. In the case of spin $I = 3/2$, these are known as the echo and antiecho pathways, respectively, as the spin echo formed by refocusing of the second-order quadrupolar broadening moves either forward (the echo) or backward (the antiecho) through the t_2 period as t_1 increases. For spin $I = 5/2$ nuclei, this behaviour is reversed and $0 \to +3 \to -1$ is the echo pathway and $0 \to -3 \to -1$ is the antiecho pathway. Neither of these experiments yields pure-phase two-dimensional lineshapes, however; instead, they yield lineshapes containing inseparable double-dispersion and double-absorption contributions (the dreaded "phase-twist" lineshape). The first attempt to overcome this problem saw the use of a two-pulse MQMAS experiment where the phase cycling allows both the echo and antiecho pathways in Fig. 1a to be recorded simultaneously, i.e., $0 \to \pm 3 \to -1$ [15]. If the two pathways have equal magnitude then the resulting time-domain data is amplitude modulated as a function of t_1 and pure-phase lineshapes can be obtained by hypercomplex Fourier transformation. Such an experiment is effective as a route to pure-phase lineshapes for spin $I = 3/2$ nuclei because a pulse with duration $\tau_p = (4\nu_1)^{-1}$, where $\nu_1 = |\gamma B_1|/2\pi$, performs the $-3 \to -1$ and $+3 \to -1$ conversions with equal efficiency. However, for spin $I > 3/2$ nuclei equal conversion of the two pathways cannot be achieved whatever the pulse duration and hence this experiment has not been widely used.

The three-pulse z-filter [16] and whole-echo MQMAS experiments [17–19] were developed to allow pure-phase lineshapes to be obtained for all spin quantum numbers. The z-filter experiment yields pure-phase two-dimensional lineshapes by acquiring data from the echo and antiecho pathways simultaneously and combining them via a population state (z magnetization) [16,20] before subsequent conversion to central-transition coherence, i.e., $0 \to \pm 3 \to 0 \to -1$. As it yields amplitude-modulated data (for all pulse durations, because the $+3 \to 0$ and $-3 \to 0$ conversions are always equally efficient), the z-filter experiment requires use of the States–Haberkorn–Ruben or TPPI methods to discriminate the sense of precession in t_1 [19]. The phase-modulated whole-echo experiment in Fig. 1b features the addition of both a third pulse and a central-transition echo period to the original two-pulse MQMAS experiment, i.e., $0 \to +3 \to +1 \to -1$. This enables acquisition of a symmetrical echo signal in t_2 for all values of t_1 and so allows pure-phase lineshapes to be obtained by complex Fourier transformation [18,19]. As it yields phase-modulated data as a function of t_1, this whole-echo experiment does not require use of either the States–Haberkorn–Ruben or TPPI methods. In our experience, phase-modulated whole-echo experiments are preferable to the alternative amplitude-modulated whole-echo experiments [17], i.e., $0 \to \pm 3 \to +1 \to -1$, as they are compatible with a split-t_1 approach and hence can utilize shorter central-transition echo periods [19].

As found with simple pulses, techniques aimed at improving the conversion step in MQMAS generally yield greater efficiency for $-3 \to -1$ or $+3 \to +1$ conversions (i.e., those with $|\Delta p| = 2$) than they do for $\pm 3 \to 0$ conversions (i.e., those with $|\Delta p| = 3$) or for $-3 \to +1$ or $+3 \to -1$ conversions (i.e., those with $|\Delta p| = 4$). For example, windowless FAM pulses consisting of two consecutive hard pulses distinguished only by a 180° phase shift have been used in the $-3 \to -1$ two-pulse and whole-echo experiments to enhance coherence transfer efficiency but are of little use in enhancing the $\pm 3 \to 0$ conversions used in the z-filter experiment [12]. In order to obtain similar signal intensity from $-3 \to +1$ or $+3 \to -1$ conversions as from the corresponding $|\Delta p| = 2$ conversions, it is possible to append a soft pulse acting as a selective 180° pulse on the central-transition to a simple or FAM pulse, as shown in Fig. 2a.

It has been reported that the two versions of the SPAM pulse, the one designed for $\pm 3 \to \pm 1$ transfer and the one designed for $\pm 3 \to \mp 1$ transfer, when implemented into the echo and antiecho versions of the two-pulse MQMAS experiment, yield very similar signal intensities [8]. In fact, this is unsurprising since the two versions of the SPAM pulse differ by a selective 180° rotation on the central-transition, i.e., the same difference as that between a FAM

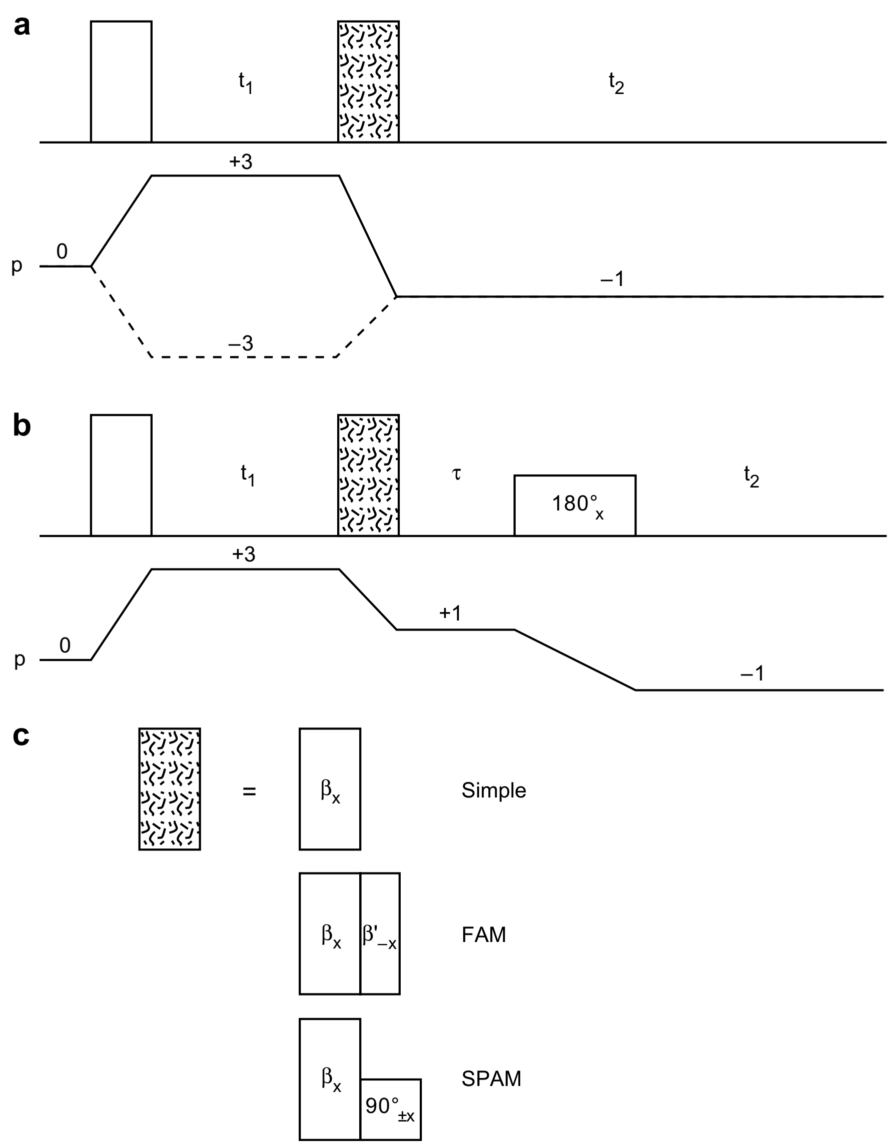

Fig. 1. (a) Simple two-pulse sequence for the (triple-quantum) MQMAS experiment. Phase cycling can be used to select either the $0 \to -3 \to -1$ or the $0 \to +3 \to -1$ coherence transfer pathway as shown, or it can be used to select both of these pathways simultaneously ($0 \to \pm 3 \to -1$). (b) Phase-modulated version of the whole-echo (triple-quantum) MQMAS experiment. (c) The conversion pulse (shaded) in (a) and (b) can be either a simple pulse, a FAM (composite) pulse, or a SPAM (composite) pulse, as shown. The two components of the SPAM pulse have the opposite phase for $\pm 3 \to \pm 1$ transfer and the same phase for $\pm 3 \to \mp 1$ transfer.

pulse and a FAM pulse with the addition of a selective 180° pulse on the central-transition (see Fig. 2b). This property opens up the possibility of using SPAM pulses to obtain pure-phase lineshapes in two-dimensional MQMAS experiments by a different method to those described so far. If SPAM pulses do give very similar signal intensities when implemented in the $-3 \to -1$ and $+3 \to -1$ two-pulse MQMAS experiments then addition of the resultant non-pure-phase spectra should yield a pure-phase spectrum [8].

The SPAM method is sometimes described as being derived from the *z*-filter experiment: the phase cycling that normally selects the $p = 0$ state after the second pulse is omitted, i.e., $0 \to \pm 3 \to \{\text{all } p\} \to -1$, hence allowing more signal through to the receiver [7,8]. In our opinion, this is a not particularly helpful description. Coherence transfer pathways [21] were introduced to specify the phase cycle that must be used in an NMR experiment. To us, it seems no more meaningful to draw all possible pathways as existing between the hard and soft pulse elements of a SPAM pulse than it is to draw them in between the two hard pulses in a FAM pulse—or, say, at the midpoint of a single hard pulse. Instead, we think of SPAM pulses as we do of FAM pulses, as composite pulses that may be used instead of a single MQMAS conversion pulse, as shown in Fig. 1c.

3. Experimental details

The NMR spectra in this paper were obtained on a Bruker Avance spectrometer equipped with a widebore 9.4 T

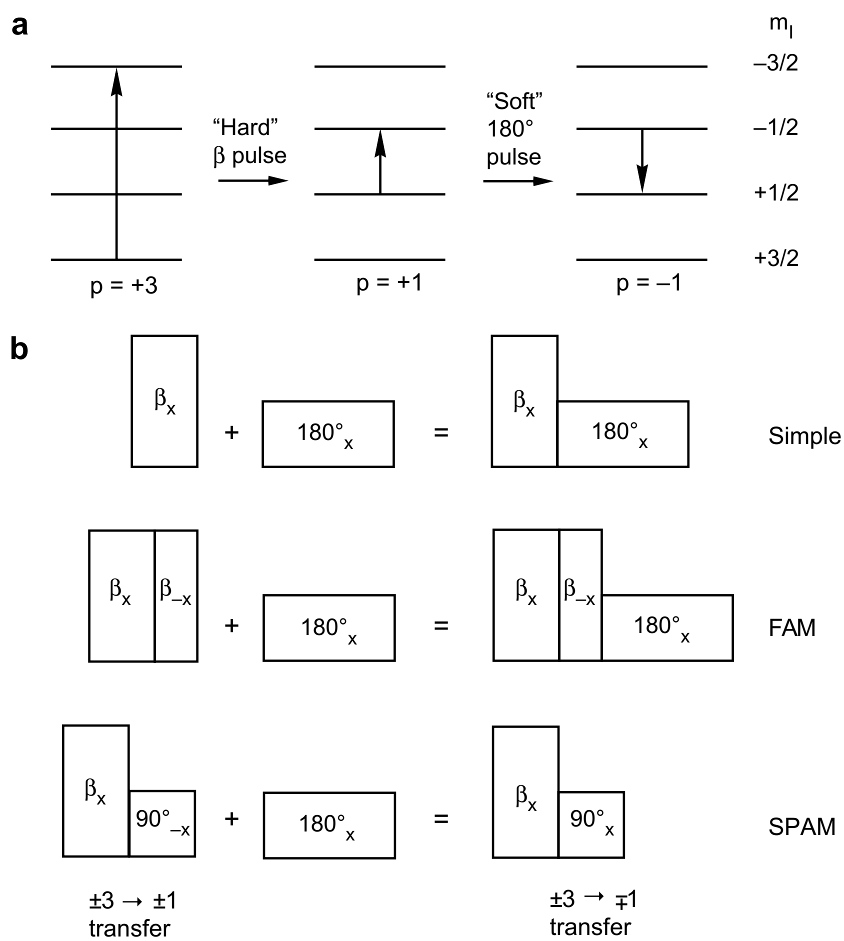

Fig. 2. (a) Any pulse that achieves $\pm3 \rightarrow \pm 1$ transfer with high efficiency can be converted into one that achieves $\pm3 \rightarrow \mp1$ transfer with approximately the same high efficiency by appending a soft pulse that acts as a selective 180° pulse on the central-transition. (b) This principle can be applied to simple, FAM and SPAM pulses, with the latter explaining the relationship between the two types ($\pm3 \rightarrow \pm 1$ and $\pm3 \rightarrow \mp1$) of SPAM pulse.

magnet. The following powdered materials were studied: (i) rubidium nitrate, $RbNO_3$, for ^{87}Rb ($I = 3/2$) NMR at a Larmor frequency of 130.9 MHz; (ii) aluminium acetylacetonate, Al(acac)$_3$, for ^{27}Al ($I = 5/2$) NMR at a Larmor frequency of 104.3 MHz and (iii) bayerite, α-Al(OH)$_3$, for ^{27}Al NMR. Materials (i) and (ii) were packed in 2.5-mm rotors and MAS rates of 20 kHz were used; (iii) was packed in a 4-mm rotor and a MAS rate of 10 kHz was used. Further experimental details may be found in the figure captions.

4. Results and discussion

Figs. 3a and b show ^{87}Rb NMR spectra of rubidium nitrate and ^{27}Al NMR spectra of aluminium acetylacetonate recorded using one-dimensional versions (i.e., with $t_1 \approx 0$) of the two-pulse MQMAS experiment in Fig. 1a. Either a simple, FAM or SPAM pulse was used for the conversion pulse as shown, while either the coherence transfer pathway $0 \rightarrow -3 \rightarrow -1$ or $0 \rightarrow +3 \rightarrow -1$ was selected by phase cycling as shown. It can be seen that FAM pulses appear to yield the most signal intensity for both spin $I = 3/2$ and 5/2. SPAM pulses yield a smaller, but still useful, enhancement relative to the simple pulse, while the two versions of the SPAM pulse yield very similar, but not identical, signal intensities for the $-3 \rightarrow -1$ and $+3 \rightarrow -1$ pathways. These experimental results are supported by the spin $I = 3/2$ computer simulations in Fig. 3c.

Fig. 4 presents two-dimensional ^{87}Rb MQMAS NMR spectra of rubidium nitrate. The spectra in Figs. 4a and b were recorded using a split-t_1 version of the whole-echo experiment in Fig. 1b [19] with either a simple (Fig. 4a) or FAM (Fig. 4b) conversion pulse. A split-t_1 whole-echo experiment was also recorded with a SPAM conversion pulse (not shown) and yielded a similar result. The spectra in Figs. 4c and d were recorded using a two-pulse MQMAS experiment with a $-3 \rightarrow -1$ SPAM and a $+3 \rightarrow -1$ SPAM conversion pulse, respectively, while the spectrum in Fig. 4e is the sum of these two. The spectrum in Fig. 4f was recorded using a z-filter experiment. It can be seen that the whole-echo experiments yield absorption-mode two-dimensional lineshapes, as does the z-filter and the combination of the two SPAM experiments. As expected,

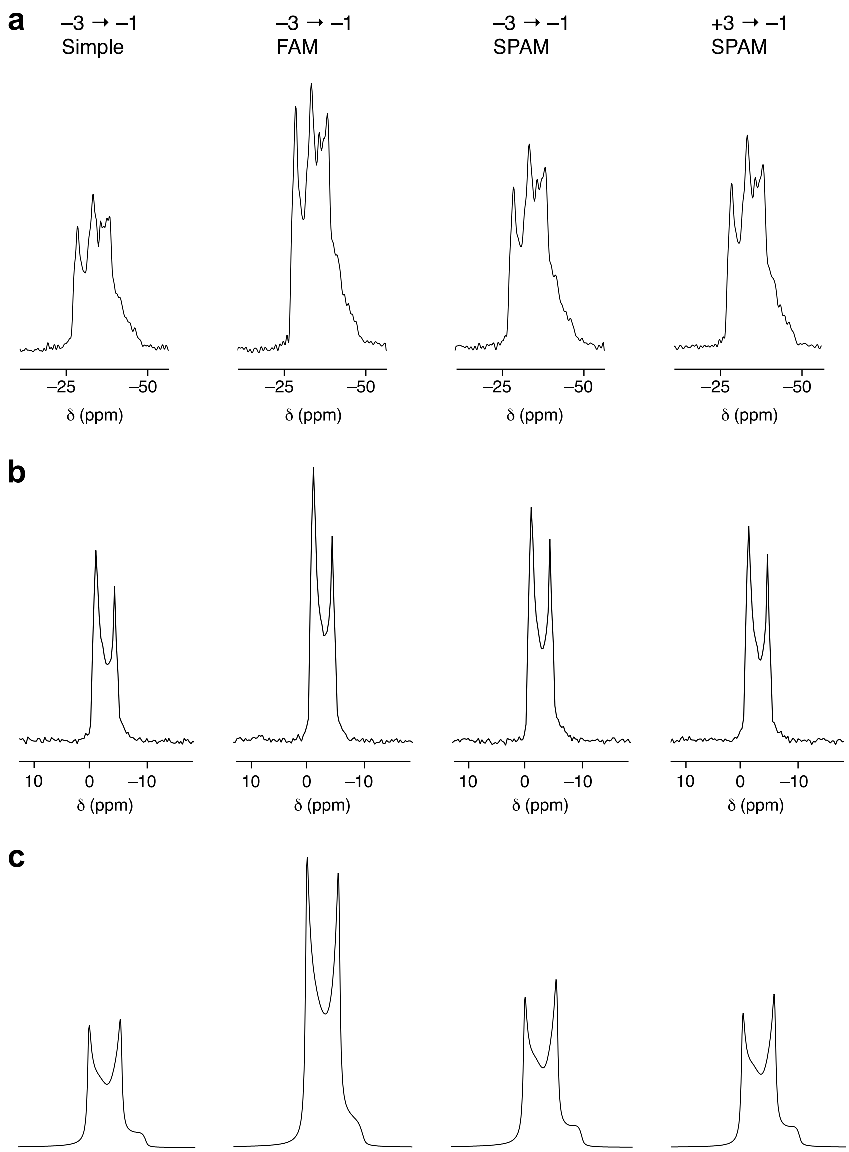

Fig. 3. (a) ^{87}Rb NMR spectra of $RbNO_3$, (b) ^{27}Al NMR spectra of Al(acac)$_3$, and (c) spin $I = 3/2$ computer-simulated spectra recorded or generated using one-dimensional versions of the two-pulse MQMAS experiment in Fig. 1a using the conversion pulses and coherence transfer pathways shown. Experimental/simulation parameters: (a) 2.9 μs excitation pulse (corresponding to hard-pulse radiofrequency field strength of ~150 kHz), 0.9 μs simple conversion pulse, 1.3 μs + 0.75 μs FAM pulse, 1.3 μs + 13.7 μs ($\nu_1 \approx 9.1$ kHz) SPAM pulse; (b) 4.0 μs excitation pulse (corresponding to a hard-pulse radiofrequency field strength of ~100 kHz), 1.1 μs simple conversion pulse, 1.6 μs + 0.9 μs FAM pulse, 1.7 μs + 21 μs ($\nu_1 \approx 4.0$ kHz) SPAM pulse; (c) 100 MHz Larmor frequency, 2.0 MHz quadrupolar coupling constant, 150 kHz hard-pulse radiofrequency field strength, 4.5 μs excitation pulse, 1.0 μs simple conversion pulse, 1.3 μs + 0.8 μs FAM pulse, 1.2 μs + 12.5 μs ($\nu_1 = 10$ kHz) SPAM pulse.

however, the individual SPAM-echo ($-3 \rightarrow -1$) and SPAM-antiecho ($+3 \rightarrow -1$) experiments both yield phase-twist lineshapes and are thus unsuitable for high-resolution NMR spectroscopy.

Fig. 5 shows δ_2 projections of the four spectra in Fig. 4 that yield absorption-mode lineshapes, i.e., those in Figs. 4a, b, e, and f, plus that of the split-t_1 whole-echo experiment recorded with a SPAM conversion pulse. It can be seen that, while the noise level is similar in all spectra, the whole-echo experiment with either a FAM or, to a lesser extent, a SPAM conversion pulse yields the most signal. The simple whole-echo experiment and the sum of the SPAM-echo and SPAM-antiecho spectra yield significantly less signal, with the z-filter experiment yielding the lowest signal intensity of all. These results are broadly in accord with the predictions of Table 1 in Ref. [8], although they show that the additional term included there to allow for transverse relaxation in the whole-echo experiments is negligible for ^{87}Rb NMR of $RbNO_3$.

To consider the application of SPAM and FAM pulses to MQMAS NMR of amorphous or disordered materials [22], ^{27}Al NMR experiments were performed on bayerite, α-Al(OH)$_3$. This material features Al in an octahedrally coordinated environment, with a single ^{27}Al peak appearing at $\delta \sim 0$ ppm and exhibiting features characteristic of the presence of distributions of chemical

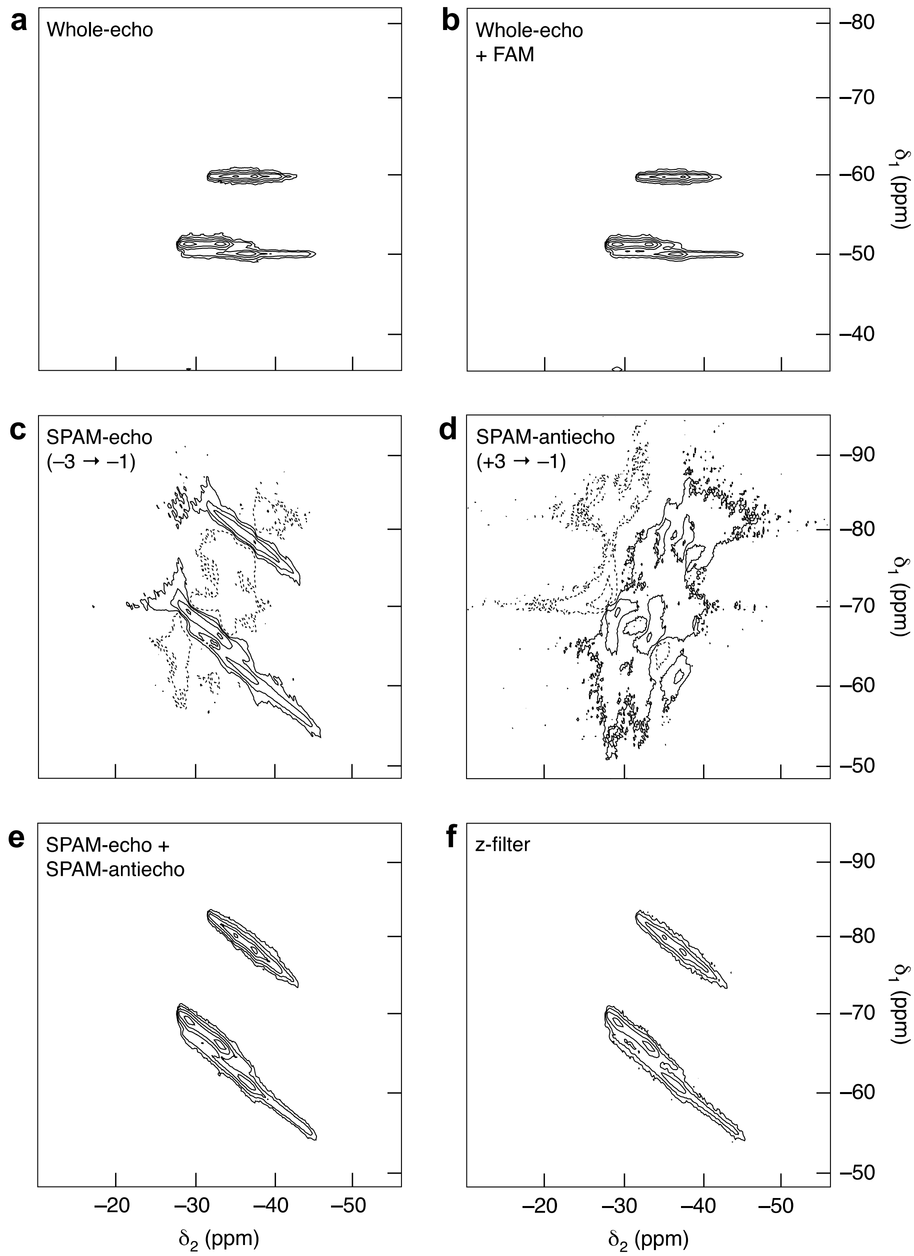

Fig. 4. Two-dimensional ^{87}Rb MQMAS NMR spectra of $RbNO_3$ obtained (a) using a split-t_1 version of the whole-echo experiment in Fig. 1b with a simple conversion pulse, (b) using a split-t_1 version of the whole-echo experiment in Fig. 1b with a FAM conversion pulse, (c) using the two-pulse experiment in Fig. 1a with a $-3 \rightarrow -1$ SPAM conversion pulse, (d) using the two-pulse experiment in Fig. 1a with a $+3 \rightarrow -1$ SPAM conversion pulse, (e) by summing (c) and (d), and (f) using a *z*-filter experiment. Experimental parameters: (a and b) 96 transients (duration 20.6 ms) averaged for each of 256 t_1 increments; (c and d) 48 transients averaged for each of 256 t_1 increments; (f) 48 transients averaged for each of 512 t_1 increments (TPPI method). The maximum duration of the triple-quantum evolution period was the same in each experiment and the spectra in (a, b, e, and f) were recorded in the same total experiment time. All pulse durations were carefully optimized.

shift and quadrupolar parameters [23]. Fig. 6 shows the results of the same series of one-dimensional experiments as were used in Fig. 3 for the crystalline compounds. As in Fig. 3, the $-3 \rightarrow -1$ FAM pulse yields a larger enhancement than the $-3 \rightarrow -1$ SPAM pulse. However, the two versions of the SPAM pulse here yield slightly more different signal intensities for the $-3 \rightarrow -1$ and $+3 \rightarrow -1$ pathways, probably due to the presence of Al sites with a very small quadrupolar coupling constant, on which the selective 90° pulse in the SPAM composite pulse would be ineffective.

Fig. 7 shows two-dimensional ^{27}Al MQMAS NMR spectra of bayerite. The spectra in Figs. 7a and b were recorded using a two-pulse MQMAS experiment with a $-3 \rightarrow -1$ SPAM and a $+3 \rightarrow -1$ SPAM conversion pulse, respectively, while the spectrum in Fig. 7c is the sum of these two. The spectrum in Fig. 7d was recorded using a *z*-filter experiment. As in Fig. 4, the individual SPAM-anti-

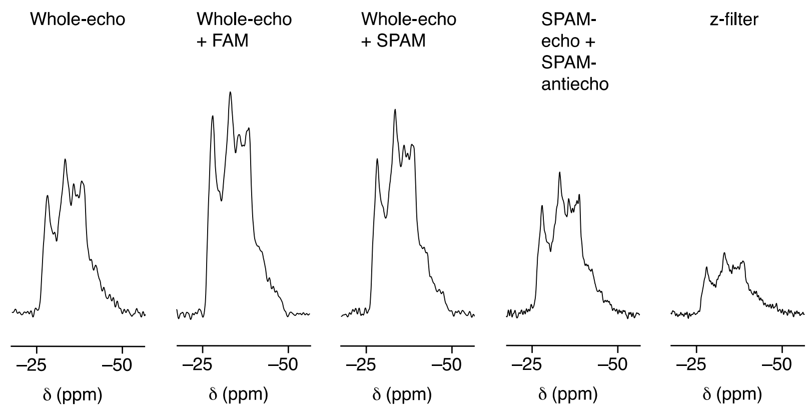

Fig. 5. δ_2 projections of the four spectra in Fig. 4 that yield absorption-mode lineshapes, plus that of a split-t_1 whole-echo spectrum recorded with a SPAM conversion pulse.

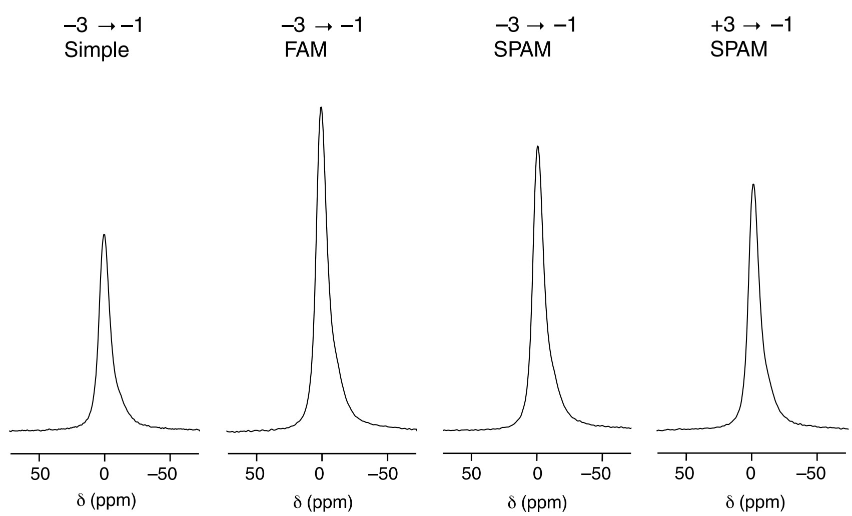

Fig. 6. ^{27}Al NMR spectra of α-Al(OH)$_3$ recorded using one-dimensional versions of the two-pulse MQMAS experiment in Fig. 1a using the conversion pulses and coherence transfer pathways shown. Experimental parameters: 2.8 μs excitation pulse (corresponding to a hard-pulse radiofrequency field strength of ~150 kHz), 0.9 μs simple conversion pulse, 1.5 μs + 0.8 μs FAM pulse, 1.2 μs + 12.0 μs ($\nu_1 \approx 6.9$ kHz) SPAM pulse.

echo ($-3 \rightarrow -1$) and SPAM-echo ($+3 \rightarrow -1$) experiments both yield unacceptably phase-twisted lineshapes. The *z*-filter and the combination of the two SPAM experiments both seem to yield absorption-mode two-dimensional lineshapes, although small differences between the two are apparent. It is probably not possible to say which of the lineshapes in Figs. 7c and d is closest to the "true" lineshape but, in view of the difference in signal intensities observed in Fig. 6 between the $-3 \rightarrow -1$ and $+3 \rightarrow -1$ pathways obtained with a SPAM pulse, we are inclined to have much greater confidence in the *z*-filter spectrum, despite its lower signal-to-noise ratio.

We have also evaluated the use of FAM and SPAM pulses in ^{87}Rb STMAS [2,24] and DQF-STMAS [24,25] NMR spectroscopy of rubidium nitrate (results not shown). We observed that a FAM pulse in the $+1$ (ST) $\rightarrow +1$ (CT) conversion step of a whole-echo STMAS experiment yielded about 10% more signal than a simple pulse, while SPAM pulses failed to yield any enhancement. In contrast, we found that a SPAM pulse in the $+2 \rightarrow +1$ conversion step of a whole-echo DQF-STMAS [24] experiment yielded about 40% more signal than a simple pulse, while FAM pulses failed to yield any enhancement. Because of the small loss of signal intensity associated with double-quantum filtration [24,25], we found that STMAS with FAM and DQF-STMAS with SPAM yielded essentially equal signal-to-noise ratios.

5. Conclusions

As a result of this work, we have reached the following conclusions.

(i) FAM and SPAM can both be considered as composite pulses and can be used for enhanced $\pm 3 \rightarrow \pm 1$ coherence transfer in MQMAS experiments; SPAM can be used for enhanced $\pm 3 \rightarrow \mp 1$ coherence transfer.
(ii) FAM pulses appear to yield greater signal enhancement than SPAM pulses for $\pm 3 \rightarrow \pm 1$ coherence transfer. It is likely that other methods, such as DFS or HS pulses, will outperform the FAM pulses we have used.

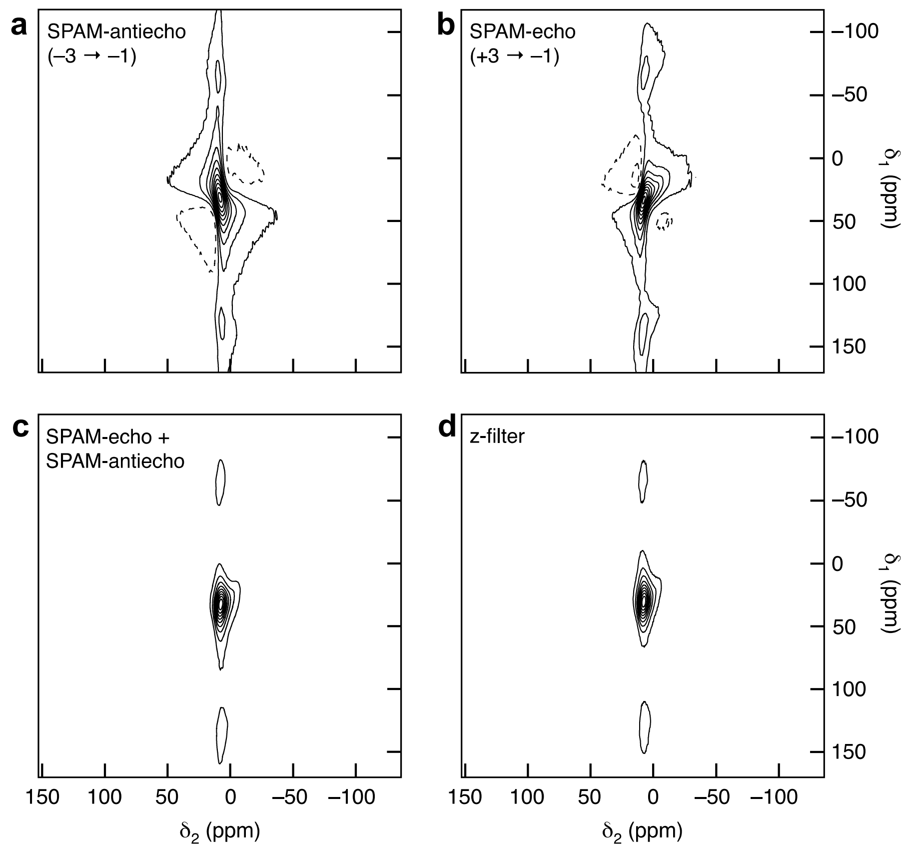

Fig. 7. Two-dimensional ^{27}Al MQMAS NMR spectra of α-$Al(OH)_3$ obtained (a) using the two-pulse experiment in Fig. 1a with a $-3 \rightarrow -1$ SPAM conversion pulse, (b) using the two-pulse experiment in Fig. 1a with a $+3 \rightarrow -1$ SPAM conversion pulse, (c) by summing (a) and (b), and (d) using a *z*-filter experiment. Experimental parameters: (a and b) 96 transients (duration 7.3 ms) averaged for each of 48 t_1 increments; (d) 96 transients averaged for each of 96 t_1 increments (TPPI method). The maximum duration of the triple-quantum evolution period was the same in each experiment and the spectra in (c and d) were recorded in the same total experiment time. All pulse durations were carefully optimized.

(iii) SPAM pulses are a useful addition to the armoury of MQMAS enhancement techniques as they require no additional experimental optimization when compared with a simple conversion pulse (since a soft pulse is always calibrated for use elsewhere in both the *z*-filter and whole-echo methods); in contrast, the FAM pulses used here require iterative optimization of two hard pulses.

(iv) The two versions of the SPAM pulse, the one designed for $\pm3 \rightarrow \pm1$ transfer and the one designed for $\pm3 \rightarrow \mp1$ transfer, yield similar, but not identical, signal intensities.

(v) Approximately absorption-mode two-dimensional lineshapes can be obtained by adding together two-pulse MQMAS spectra obtained with $+3 \rightarrow -1$ SPAM and $-3 \rightarrow -1$ SPAM conversion pulses but, because of the non-identical signal intensities, our confidence in the quality of these lineshapes is lower than in that of lineshapes obtained by more accurate methods.

(vi) The $\pm3 \rightarrow \pm1$ FAM and SPAM pulses are ideally suited to inserting into phase-modulated whole-echo MQMAS methods and, when used in this way, appear generally to yield high-quality absorption-mode lineshapes and a significantly higher signal-to-noise ratio than the addition of SPAM-echo and SPAM-antiecho spectra.

(vii) Absorption-mode MQMAS lineshapes are not obtained with the SPAM-echo and SPAM-antiecho experiments on their own and these methods are thus unsuitable for high-resolution NMR spectroscopy. A suggestion in the literature [8] that nearly absorption-mode lineshapes can be obtained for amorphous or disordered materials using the SPAM-echo experiment alone is not supported by our results.

(viii) The $\pm2 \rightarrow \pm1$ SPAM pulse appears to be a very effective way of enhancing the intensity of phase-modulated whole-echo DQF-STMAS spectra.

(ix) Overall, considering both MQMAS and STMAS (including the DQF-STMAS variant), we generally favour the use of phase-modulated whole-echo experiments. Where appropriate, and if desired, FAM, SPAM, DFS or HS pulses may be easily used in these experiments. However, in the (rare, in our experience) case that the central-transition T_2 relaxation time is very short or the (much more common) case that there are wide distributions of second-order quadrupolar broadenings and T_2 time constants (as is frequently found, for example, in amorphous or disordered materials) we would recommend instead the MQMAS or STMAS *z*-filter experiments as by far the most robust methods of obtaining undistorted absorption-mode two-dimensional lineshapes. The addition of fully acquired SPAM-echo and SPAM-antiecho spectra is a possible alternative in these two cases, and will yield a higher signal-to-noise ratio than the *z*-filter, but our results suggest that some caution may need to be exercised in the interpretation of the resulting lineshapes.

Acknowledgments

We are grateful to EPSRC for a studentship (T.J.B.) and to Dr. Sharon E. Ashbrook (St. Andrews, UK) for a careful reading of the manuscript.

References

[1] L. Frydman, J.S. Harwood, Isotropic spectra of half-integer quadrupolar spins from bidimensional magic-angle-spinning NMR, J. Am. Chem. Soc. 117 (1995) 5367–5368.
[2] Z. Gan, Isotropic NMR spectra of half-integer quadrupolar nuclei using satellite transitions and magic-angle spinning, J. Am. Chem. Soc. 122 (2000) 3242–3243.
[3] G. Wu, D. Rovnyak, R.G. Griffin, Quantitative multiple-quantum magic-angle-spinning NMR spectroscopy of quadrupolar nuclei in solids, J. Am. Chem. Soc. 118 (1996) 9326–9332.
[4] A.P.M. Kentgens, R. Verhagen, Advantages of double frequency sweeps in static, MAS and MQMAS NMR of spin $I = 3/2$ nuclei, Chem. Phys. Lett. 300 (1999) 435–443.
[5] P.K. Madhu, A. Goldburt, L. Frydman, S. Vega, Sensitivity enhancement of the MQMAS NMR experiment by fast amplitude modulation of the pulses, Chem. Phys. Lett. 307 (1999) 41–47.
[6] R. Siegel, T.T. Nakashima, R.E. Wasylishen, Sensitivity enhancement of MQMAS NMR spectra of spin 3/2 nuclei using hyperbolic secant pulses, Chem. Phys. Lett. 403 (2005) 353–358.
[7] Z. Gan, H.T. Kwak, Enhancing MQMAS sensitivity using signals from multiple coherence transfer pathways, J. Magn. Reson. 168 (2004) 346–351.
[8] J.P. Amoureux, L. Delevoye, S. Steuernagel, Z. Gan, S. Ganapathy, L. Montagne, Increasing the sensitivity of 2D high-resolution NMR methods applied to quadrupolar nuclei, J. Magn. Reson. 172 (2005) 268–278.
[9] J.P. Amoureux, A. Flambard, L. Delevoye, L. Montagne, A very sensitive high-resolution NMR method for quadrupolar nuclei: SPAM–DQF-STMAS, Chem. Commun. (2005) 3472–3474.
[10] J.P. Amoureux, L. Delevoye, G. Fink, F. Taulelle, A. Flambard, L. Montagne, Implementing SPAM into STMAS: a net sensitivity improvement in high-resolution NMR of quadrupolar nuclei, J. Magn. Reson. 175 (2005) 285–299.
[11] J.W. Wiench, G. Tricot, L. Delevoye, J. Trebosc, J. Frye, L. Montagne, J.P. Amoureux, M. Pruski, SPAM-MQ-HETCOR: an improved method for heteronuclear correlation spectroscopy between quadrupolar and spin-1/2 nuclei in solid-state NMR, Phys. Chem. Chem. Phys. 8 (2006) 144–150.
[12] A. Goldbourt, P.K. Madhu, S. Vega, Enhanced conversion of triple to single-quantum coherence in the triple-quantum MAS NMR spectroscopy of spin-5/2 nuclei, Chem. Phys. Lett. 320 (2000) 448–456.
[13] M.H. Levitt, R. Freeman, NMR population inversion using a composite pulse, J. Magn. Reson. 33 (1979) 473–476.
[14] S. Wimperis, Broadband, narrowband, and passband composite pulses for use in advanced NMR experiments, J. Magn. Reson. A 109 (1994) 221–231.
[15] C. Fernandez, J.P. Amoureux, Triple-quantum MAS NMR of quadrupolar nuclei, Solid State NMR 5 (1996) 315–321.
[16] J.P. Amoureux, C. Fernandez, S. Steuernagel, Z filtering in MQMAS NMR, J. Magn. Reson. A 123 (1996) 116–118.
[17] D. Massiot, B. Touzo, D. Trumeau, J.P. Coutures, J. Virlet, P. Florian, P.J. Grandinetti, Two-dimensional magic-angle spinning isotropic reconstruction sequences for quadrupolar nuclei, Solid State NMR 6 (1996) 73–83.
[18] S.P. Brown, S. Wimperis, Two-dimensional multiple-quantum MAS NMR of quadrupolar nuclei. Acquisition of the whole echo, J. Magn. Reson. 124 (1997) 279–285.
[19] S.P. Brown, S. Wimperis, Two-dimensional multiple-quantum MAS NMR of quadrupolar nuclei: a comparison of methods, J. Magn. Reson. 128 (1997) 42–61.
[20] S.P. Brown, S.J. Heyes, S. Wimperis, Two-dimensional MAS multiple-quantum NMR of quadrupolar nuclei. Removal of inhomogeneous second-order broadening, J. Magn. Reson. A 119 (1996) 280–284.
[21] G. Bodenhausen, H. Kogler, R.R. Ernst, Selection of coherence-transfer pathways in NMR pulse experiments, J. Magn. Reson. 58 (1984) 370–388.
[22] J. McManus, S.E. Ashbrook, K.J.D. MacKenzie, S. Wimperis, ^{27}Al multiple-quantum MAS and ^{27}Al{^{1}H} CPMAS NMR study of amorphous aluminosilicates, J. Non-Cryst. Solids 282 (2001) 278–290.
[23] S.E. Ashbrook, K.J.D. MacKenzie, S. Wimperis, ^{27}Al multiple-quantum MAS NMR of mechanically treated bayerite (α-Al(OH)$_3$) and silica mixtures, Solid State NMR 20 (2001) 87–99.
[24] S.E. Ashbrook, S. Wimperis, High-resolution NMR of quadrupolar nuclei in solids: the satellite-transition magic angle spinning (STMAS) experiment, Prog. NMR Spectrosc. 45 (2004) 53–108.
[25] H.T. Kwak, Z. Gan, Double-quantum filtered STMAS, J. Magn. Reson. 164 (2003) 369–372.